Intramolecular Interactions in the Ground and Excited State of Tetrakis(*N*-methylpyridyl)porphyrins

Frank J. Vergeldt,* Rob B. M. Koehorst, Arie van Hoek, and Tjeerd J. Schaafsma

Department of Molecular Physics, Agricultural University, Dreijenlaan 3, 6703 HA Wageningen, The Netherlands

Received: May 18, 1994; In Final Form: December 13, 1994[⊗]

The fluorescent properties of the cationic free base tetrakis(4-*N*-methylpyridyl)porphyrin (H_2TMPyP(4)) in aqueous solution have been the subject of considerable discussion. Conclusions by various authors on the presence of homo-aggregation of H_2TMPyP in these solutions are contradictory. The present work reports spectroscopic data for three isomers of H_2TMPyP(n) (n = 2, 3, or 4) at varying concentrations, solvent polarity, and temperature. ^{1}H NMR spectra of H_2TMPyP(4) show no ground-state monomers below 10^{-3} M in water. Fluorescence spectra of the three isomers in aqueous solutions indicate the absence of aggregates both in the ground and excited state. Fluorescence lifetimes of the three isomers both in solution as well as adsorbed on solid surfaces can be explained by taking into account their dependence on the steric hindrance for rotation of the pyridinium groups of the three isomers with respect to the porphyrin macrocycle. Molecular mechanics confirms a higher degree of steric hindrance of H_2TMPyP(2) as compared to the two other isomers. From the experimental results it is concluded that the first excited singlet state S_1 of the porphyrin mixes with a nearby CT state slightly above this S_1 state. In this CT state an electron is transferred from the porphyrin macrocycle to the pyridinium group. The amount of S_1–CT mixing, responsible for the spectroscopic differences, is determined by the degree of coplanarity and resonance interaction of the porphyrin and the pyridinium π-systems, and by the solvent polarity which determines the energy difference between the two states.

Introduction

Anionic tetrakis(4-carboxyphenyl)porphyrins (TCPP(4)) and cationic tetrakis(4-*N*-methylpyridyl)porphyrins (TMPyP(4)) form 1:1 heterodimers in water/methanol (4:1 v/v) in high yield. Upon optical excitation, these dimers exhibit ultrafast charge separation and fast charge recombination.[1–3] In view of their geometry and spectroscopic properties, the dimers can be viewed as models for the dimeric primary donor of bacterial photosynthetic reaction centers.[4,5]

Being noncovalently bound, precise knowledge of the extent of homo-aggregation in aqueous solutions of both dimer constituents is crucial for a correct interpretation of the results from transient absorption experiments for heterodimer solutions. Homo-aggregates of TCPP, anionic tetrakis(4-sulfonatophenyl)-porphyrins (TSPP), and cationic tetrakis(4-(trimethylammono)-phenyl)porphyrins (TMAPP) are easily formed in aqueous solutions.[6–8] Conclusions about the aggregation of the three isomers of free base tetrakis(*N*-methylpyridyl)porphyrins (H_2TMPyP) (Figure 1) by various authors[6,7,9–16] are contradictory which prompted us to further investigations, reported in this paper.

Pasternack *et al.*[6,7] and others[17] concluded that the free base Ni(II), Cu(II), and Zn(II) complexes of H_2TMPyP(4) do not form concentration dimers nor do they aggregate in the presence of inorganic salts. This conclusion was based on the absence of any detectable deviation from Lambert–Beer's law upon dilution and on temperature-jump relaxation experiments. Later Kano *et al.*[10,11] concluded from steady-state fluorescence spectra, that ground-state dimers of H_2TMPyP(4) are present in water even at concentrations as low as 10^{-7} M. Upon addition of methanol, surfactants, or charged or uncharged aromatic compounds, and upon increase of temperature or dilution of aqueous solutions below 10^{-7} M, the single, almost structureless fluorescence band resolves into the usual porphyrin fluorescence spectrum with two well-resolved vibrational bands. Brookfield *et al.*[13] confirmed these results demonstrating a deviation from Lambert–Beer's law and a small red shift of the Soret band upon decreasing the concentration of H_2TMPyP(4) from 10^{-5} to 10^{-7} M. Pasternack *et al.*[12] criticized these results in view of their ^{1}H NMR results for H_2TMPyP(4) and its complexation with nucleosides and nucleotides. This criticism was replied with new ^{1}H NMR results and other spectroscopic data which were claimed to support the existence of ground-state dimers of H_2TMPyP(4). Kadish *et al.*[15] concluded from ^{1}H NMR and EPR data that there is no evidence for a ground-state monomer–aggregate equilibrium of H_2TMPyP(4) in the 10^{-3}–10^{-4} M

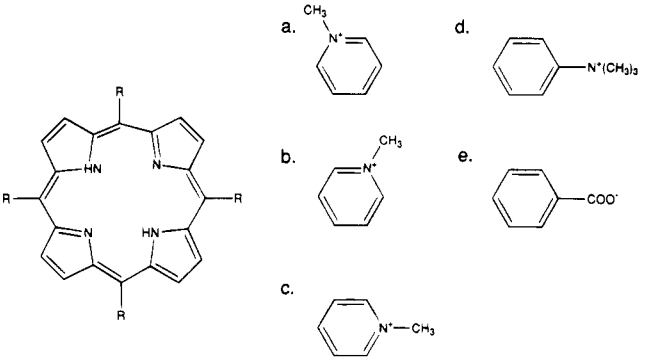

Figure 1. Molecular structure of the three isomers of the free base tetrakis(*N*-methylpyridyl)porphyrins H_2TMPyP: (a) tetrakis(2-*N*-methylpyridyl)porphyrin (H_2TMPyP(2)); (b) tetrakis(3-*N*-methylpyridyl)-porphyrin (H_2TMPyP(3)); (c) tetrakis(4-*N*-methylpyridyl)porphyrin (H_2TMPyP(4)); (d) tetrakis(4-(trimethylammono)phenyl)porphyrin (H_2-TMAPP); (e) tetrakis(4-carboxyphenyl)porphyrin (H_2TPPC). For metalloporphyrins, both protons are replaced by metal ions.

* Author to whom correspondence should be addressed.

[⊗] Abstract published in *Advance ACS Abstracts,* February 15, 1995.

0022-3654/95/2099-4397$09.00/0

concentration range. From fluorescence kinetics Kemnitz *et al.*[16] calculated a homodimerization constant of 8.8×10^5 M^{-1} in disagreement with the values predicted by the models of Pasternack and Kano, respectively.

This paper presents detailed results on the above mentioned issues for the three isomers H_2TMPyP at various porphyrin concentrations, solvent polarity, and temperature, using optical spectroscopy and ^{1}H NMR. It is shown that the controversial results, reported by a number of authors, can be explained by taking the adsorption of H_2TMPyP onto solid surfaces or solid impurities into account. Under carefully controlled conditions, no evidence is found that the observed anomalous fluorescence spectra and fluorescence lifetimes of the three isomers H_2TMPyP are due to ground- or excited-state dimerization. All of the observed H_2TMPyP spectroscopic features can be explained by a model, invoking the formation of an intramolecular exciplex state with a charge-transfer admixture depending on the solvent polarity as well as on the rotational freedom of the pyridinium side groups in the various H_2TMPyP isomers.

TMPyP(4) has been widely used as an antitumour reagent in photodynamic therapy, involving complexation of porphyrin and DNA.[18-21] The results of this work may also shed some new light on the nature and role of the TMPyP excited state in forming the porphyrin−DNA exciplex, thought to be the active component in the photodynamic process.[22-24]

Experimental Section

Cationic H_2TMPyP(3) and H_2TMPyP(4) (Figure 1) were synthesized as their iodide salts from the precursors free base tetrakis(3-*N*-pyridyl)porphyrin and free base tetrakis(4-*N*-pyridyl)porphyrin by reaction with methyl iodide. The three isomers of H_2TMPyP including H_2TMPyP(2) (Figure 1) were obtained as their chloride salts from Midcentury Chemicals (Posen, IL) and used as received. Chloride salts of H_2TMPyP(3) and H_2TMPyP(4) were also made by passing the aqueous solution of H_2TMPyP(3)I_4 and H_2TMPyP(4)I_4 over an anion exchange column (Amberlite IRA-400, E. Merck, Darmstadt, Germany) in the chloride form. The iodide salts of ZnTMPyP(4), H_2TCPP, and ZnTCPP (Figure 1) were prepared as previously described.[1] The tosylate salt of H_2TMAP (Figure 1) was purchased from Aldrich Chem. Co. (Milwaukee, WI) and used as received. Optical spectra of all porphyrins were in good agreement with published data.[25]

UV/vis absorption spectra were measured using a Kontron Uvikon 810 spectrophotometer. Steady-state fluorescence spectra were recorded with a Perkin-Elmer LS-5 spectrometer and corrected for the characteristics of the detection monochromator and photomultiplier by a spectral irradiation standard (1000 W Fel type lamp, Eppley Lab. Inc., Newport, KY). For all fluorescence spectra the excitation wavelength was chosen at the maximum of the $Q_y(0,1)$ absorption band (see Table 1). Fluorescence spectra were fitted to Gaussian functions using a graphics and data analysis package (Igor, WaveMetrics, Lake Oswego, OR).

Since we found that material adsorbing at the cuvette walls may complicate spectroscopic experiments, all steady-state experiments were performed immediately after dilution, in plastic cuvettes with a 1 cm optical path length (Sarstedt, Germany) using freshly prepared stock solutions.

Fluorescence lifetimes were determined using the time-correlated single photon counting technique.[26] For excitation of the sample the output of a mode-locked CW Nd:YLF laser was frequency doubled, resulting in light pulses at 527 nm and 35 ps fwhm. Using an electrooptic modulator setup in a dual pass arrangement[27] the repetition rate of the excitation pulses was decreased to 600 kHz at an energy of about 10 pJ. Fluorescence light was detected at several wavelengths between 550 and 744 nm using Baltzers interference filters with a bandpass of about 10 nm fwhm together with a Schott KV550 cutoff filter. A Hamamatsu 1645 U01 microchannel plate photomultiplier was used for detection. For deconvolution of the data the reference method[26] was used with rose bengal ($\tau_{ref} = 0.55$ ns) and oxazine ($\tau_{ref} = 0.78$ ns), both in methanol, as reference compounds for the regions 635−647 nm and 657−744 nm, respectively. Each fluorescence decay was analyzed using the FAME program (Maximum Entropy Data Consultants Ltd., Cambridge, England) to find the most probable distribution of lifetimes using the maximum entropy algorithm.[28] In addition global analysis (Globals Unlimited, Urbana, IL) was applied to a series of fluorescence decays to determine the wavelength-dependent distributions of species with different lifetimes.[29,30] To exclude spurious effects of oxygen all samples were purged for 10 min with deoxygenated argon. Fluorescence lifetime measurements of porphyrin solutions were performed in 1 cm quartz cuvettes (Helma Benelux, The Hague, The Netherlands) instead of plastic cuvettes to prevent spurious background fluorescence.

FT ^{1}H NMR spectra were measured at 200 MHz on a Bruker AC300 spectrometer.

Molecular mechanics calculations were carried out using the CHARMm energy function (version 21.2) implemented in the QUANTA/CHARMm package (version 3.0, Polygen Co., Waltham, MA). Constrained minimalization was performed with 2000 steps of the Powell conjugate gradient method followed by 200 steps of the more rigorous ABNR (adopted basis-set Newton−Raphson) method, using the standard CHARMm force field. Partial charges were assigned by means of a charge template in QUANTA/CHARMm. There are no solvent molecules included in the calculation. In QUANTA/CHARMm the screening effect of water was simulated using a distant-dependent dielectric constant. This is achieved describing the electrostatic interaction by

$$E_{elec} = \sum_{i,j>i} \left(\frac{q_i q_j}{4\pi\epsilon_0 r_{ij}} \right) \frac{1}{r_{ij}} \qquad (1)$$

implying that the electrostatic interaction is weighted by the distance r_{ij} between the partial charges q_i and q_j.

TABLE 1: Positions (nm) and Relative Intensities (between Parentheses) of the Q Absorption Maxima in Water and Methanol

porphyrin	solvent	$Q_y(0,1)$	$Q_y(0,0)$	$Q_x(0,1)$	$Q_x(0,0)$
H_2TMPyP(4)	H_2O	512 (1.00)	545 (0.20)	580 (0.40)	632 (0.08)
	CH_3OH	510 (1.00)	543 (0.20)	584 (0.37)	640 (0.08)
H_2TMPyP(3)	H_2O	514 (1.00)	547 (0.17)	581 (0.37)	633 (0.04)
	CH_3OH	511 (1.00)	544 (0.18)	586 (0.33)	641 (0.04)
H_2TMPyP(2)	H_2O	518 (1.00)	554 (0.35)	585 (0.41)	638 (0.10)
	CH_3OH	515 (1.00)	549 (0.37)	589 (0.33)	646 (0.09)

Results

Absorption Spectra. Absorption spectra of the three isomers of H_2MPyP in aqueous solution agree with published data,[25] except for the $Q_x(0,0)$ band of H_2TMPyP(3) (Table 1). The published value of 640 nm for the position of the $Q_x(0,0)$ transition for H_2TMPyP(3) in water is most likely due to a chlorin formed during preparation. Changing from water to methanol results in similar shifts of the $Q_x(0,0)$ transition for H_2TMPyP(2) as for the other two isomers. A small blue shift of the Q_y bands, a small red shift of the Q_x bands, and changes in the intensity ratio of the Q(0,0) and Q(0,1) bands are observed

TABLE 2: Chemical Shift Differences $\Delta\delta$ between 1×10^{-3} M Water-Soluble Porphyrins Dissolved in D_2O with 1 M KCl and in D_2O/CD_3OD (4:1)

porphyrin	$\Delta\delta$ for H_{ortho}, ppm	$\Delta\delta$ for H_{meta}, ppm
H_2TPPC	−1.21	−0.20
ZnTPPC	−0.73	−0.20
H_2TMPyP	0.00	0.00
ZnTMPyP	0.00	0.00

for all isomers in methanol as compared to water. There is hardly any effect of temperature on the absorption spectra for the three isomers.

^{1}H NMR Spectra. Protons in the proximity of a porphyrin macrocycle exhibit large aromatic ring current shifts. From these shifts the positions of protons with respect to the porphyrin plane and thus the presence and conformations of porphyrin aggregates can be calculated.[4,31,32] Table 2 summarizes the chemical shift differences between the protons of $H_2TMPyP(4)$, H_2TPPC, and ZnTPPC dissolved in D_2O containing 1 M KCl, and in D_2O/CD_3OD (4:1). Ortho protons and to a lesser extent the meta protons of the phenyl groups of H_2-TPPC and ZnTPPC exhibit an upfield shift in D_2O/1 M KCl with respect to their resonance position in D_2O/CD_3OD (4:1) as a result of aggregation due to the shielding effect of the K^+ ions.[32] For $H_2TMPyP(4)$, however, no such shift is observed.

We investigated the temperature effect on the ^{1}H NMR spectra of $H_2TMPyP(4)$ in view of the results of Kano *et al.*,[9] who found a downfield shift of 0.6 ppm for all resonances of $H_2TMPyP(4)$ and H_2TMAPP in the temperature range 294–358 K. Although for H_2TMAPP these ^{1}H NMR experiments were carried out at 5×10^{-4} M, where mainly monomers are present according to fluorescence data, the observed shift was explained as a $\pi-\pi$ interaction between the two porphyrin moieties. Because the same effect was found for $H_2TMPyP(4)$ a similar monomer–dimer equilibrium was suggested for this compound. Using the resonance signal of naturally abundant protons in D_2O as an internal reference, it was found that all resonance positions must be corrected to compensate for the downfield shift of the reference signal (0.6 ppm) at 350 K. After this correction was applied to the spectra no downfield shift for $H_2TMPyP(4)$ remained.

Fluorescence Spectra. The fluorescence spectra of the three isomers of H_2TMPyP in water are strikingly different (Figure 2). The resolution of the Q(0,0) and Q(0,1) fluorescence bands decreases in the series $H_2TMPyP(2)$ > $H_2TMPyP(3)$ > $H_2TMPyP(4)$, as previously observed by Kalyanasundaram.[25]

Kano *et al.*[10] presented fluorescence spectra of $H_2TMPyP(2)$ in the 1×10^{-5} to 1×10^{-8} M concentration range, exhibiting an increase of resolution of the Q(0,0) and Q(0,1) bands below 1×10^{-7} M. At these concentrations the fluorescence spectrum of $H_2TMPyP(4)$ in water resembles that in methanol. The authors concluded that this porphyrin is monomeric in water at concentrations below 1×10^{-7} M. In contrast with these results we did not observe changes in fluorescence spectra of $H_2TMPyP(4)$ upon dilution down to 1×10^{-9} M in ultrapure water purified by the Milli-Q water system (Millipore Co., Molsheim, France). In water of less purity, however, the effect of dilution on the resolution of fluorescence spectra as published by Kano *et al.*[10] could be reproduced. We found that the concentration at which onset of resolution enhancement of the fluorescence spectrum is observed rises with various treatments of the water by which the particulate concentration is increased, e.g., passing over cotton-wool, paper filter, or ion exchanger. We note that $H_2TMPyP(4)$ has a high affinity to solid surfaces (e.g., glass), and that the fluorescence spectrum of adsorbed $H_2TMPyP(4)$ resembles that of the porphyrin at low concentrations in water containing trace amounts of particles. The concentration dependence of the fluorescence spectra can be fitted very well using a model which takes into account a varying porphyrin concentration and a constant concentration of an unknown impurity at which the porphyrin adsorbs. Moreover, the concentration dependence did not fit to a model describing a porphyrin monomer-dimer equilibrium.

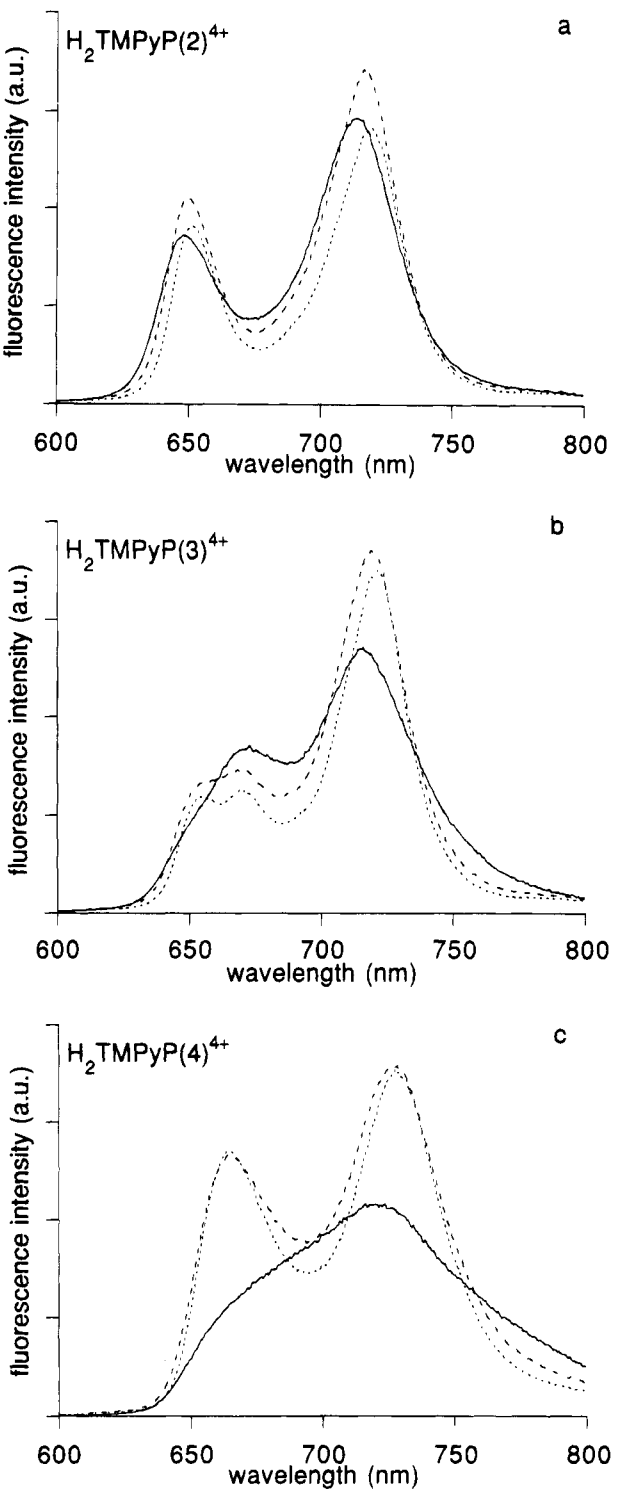

Figure 2. Fluorescence spectra of 1×10^{-5} M solutions of the three isomers of H_2TMPyP in different solvents: (—) H_2O; (– – –) H_2O/MeOH 1:1; (- - -) MeOH.

The effect of an apolar solvent (methanol) on the fluorescence spectra as compared to those in Millipore-purified water increases in the series $H_2TMPyP(2)$ < $H_2TMPyP(3)$ < $H_2TMPyP(4)$ (Figure 2). For $H_2TMPyP(4)$ a significant increase

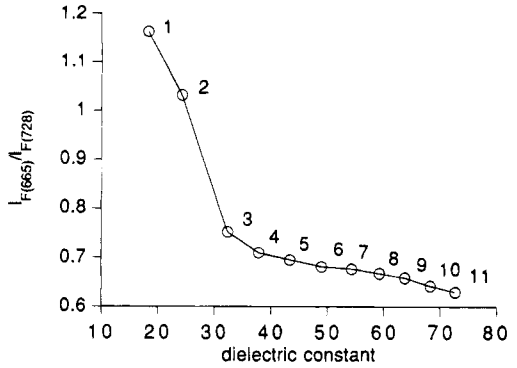

Figure 3. Ratio of ≈ 665 nm ($I_{F(665)}$) and ≈ 728 nm ($I_{F(728)}$) fluorescense intensity for $H_2TMPyP(4)(I^-)_4$ in (1) propanol; (2) ethanol (3); methanol (4); 1:9 H_2O/MeOH; (5) 1:4 H_2O/MeOH; (6) 3:7 H_2O/MeOH; (7) 2:3 H_2O/MeOH; (8) 1:1 H_2O/MeOH; (9) 3:2 H_2O/MeOH; (10) 7:3 H_2O/MeOH; (11) 4:1 H_2O/MeOH. Solvent composition is expressed as v/v ratio.

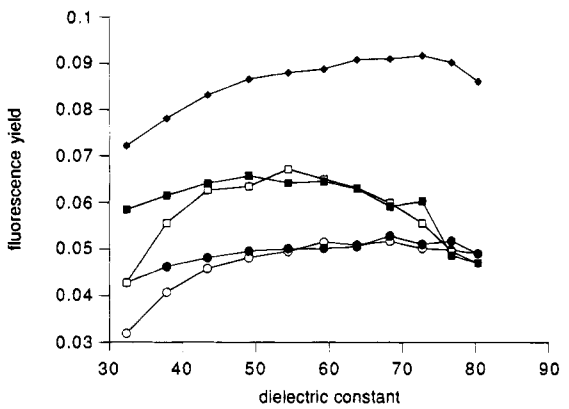

Figure 4. Relative fluorescence yield vs solvent polarity[43] for 1 × 10^{-5} M solutions of the iodide salts of $H_2TMPyP(4)$ and $H_2TMPyP(3)$ and the chloride salts of the three isomers: (◆) $H_2TMPyP(2)(Cl^-)_4$; (■) $H_2TMPyP(3)(I^-)_4$; (□) $H_2TMPyP(3)(Cl^-)_4$; (●) $H_2TMPyP(4)(I^-)_4$; (○) $H_2TMPyP(4)(Cl^-)_4$.

of resolution of the Q(0,0) and Q(0,1) bands is found in methanol. For $H_2TMPyP(3)$ and in particular for $H_2TMPyP(2)$ the spectral differences between solutions in water and methanol, respectively, are less than for $H_2TMPyP(4)$. For $H_2TMPyP(4)$ we also studied the fluorescence spectra in ethanol and propanol. For both extremes, i.e., water and propanol, the spectra have very different shapes, as is particularly reflected by the ratio of the two peaks at ≈665 and 728 nm. In Figure 3 we present the changes for intermediate cases as a function of the dielectric constant.

The effect of polarity on the fluorescence yield is shown in Figure 4. In methanol the fluorescence of porphyrins with iodide as the counterion was more strongly quenched as compared to the chloride. In water no difference in fluorescence yield was found for the two counterions.

The effect of temperature on the fluorescence spectra is shown in Figure 5. An increase of temperature increased the resolution of the fluorescence bands of $H_2TMPyP(3)$ and $H_2TMPyP(4)$ in water. The temperature dependence of the spectra of $H_2TMPyP(2)$ is much smaller than that of the $H_2TMPyP(4)$ and $H_2TMPyP(3)$ spectra. Note that the effect of increasing temperature on the resolution of the fluorescence spectra is similar to the effect of adding methanol to the aqueous solution.

Fluorescence Lifetime Measurements. Fluorescence decays of the three isomers of H_2TMPyP detected at different wavelengths between 635 and 752 nm and excited at 527 nm were recorded in H_2O, H_2O/CH_3OH 4:1, and CH_3OH (Table 3). These

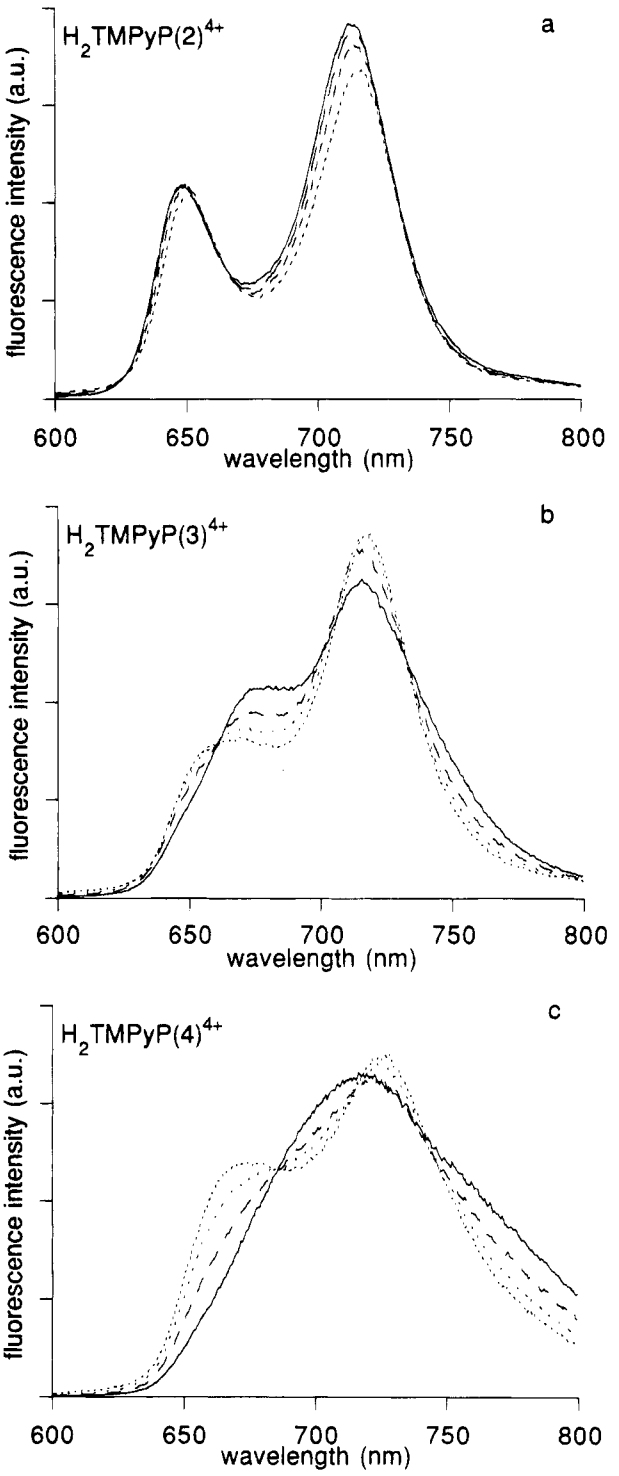

Figure 5. Effect of temperature on the fluorescence spectra of 1 × 10^{-5} M solutions of the chloride salts of the three isomers of H_2TMPyP in water: (—) 278 K; (— — —) 298 K; (— —) 318 K; (- - -) 338 K.

fluorescence decays cannot be fitted to monoexponential functions. The lifetimes of the two components are independent of the detection wavelength and the counterion for $H_2TMPyP(4)$ in H_2O/CH_3OH 4:1 (I^- or Cl^-). A third shorter component (10–40 ps) is present, but its contribution to the total fluorescence spectrum is less then 5% and therefore neglected. This component is most probably due to the use of a different solvent for the reference compound (methanol) and the porphyrin solutions.[33] In agreement with this, the amplitude of the picosecond component is smaller for solutions of the porphyrin in pure methanol.

From the fluorescence decays at different wavelengths the

TABLE 3: Lifetimes of the Fluorescence Decay of the Three Isomers of H_2TMPyP in Different Solvents

isomer	solvent	τ_1 (ns)	τ_2 (ns)
$H_2TMPyP(2)(Cl^-)_4$	H_2O	6.0	13.8
	H_2O/MeOH 4:1	5.8	14.6
	MeOH	5.0	15.2
$H_2TMPyP(3)(Cl^-)_4$	H_2O	4.3	7.9
	H_2O/MeOH 4:1	4.1	9.0
	MeOH	4.4	10.6
$H_2TMPyP(4)(I^-)_4$	H_2O/MeOH 4:1	2.7	6.6
$H_2TMPyP(4)(Cl^-)_4$	H_2O	2.7	5.1
	H_2O/MeOH 4:1	2.6	6.7
	MeOH	3.3	10.8

fluorescence spectra of the two main components of the decay were calculated, using

$$I_i(\lambda) = I_{st}(\lambda)\, A_i(\lambda)\, \tau_i \qquad (2)$$

with $I_i(\lambda)$ the spectrum of component i, $I_{st}(\lambda)$ the steady-state spectrum, $A_i(\lambda)$ the relative amplitude of component i, and τ_i its fluorescence lifetime. The lifetime-selected spectra corresponding to the longest component show the same trends as the steady-state spectra (Figure 6). Note that the spectra of the second (shorter) component show little variation but are different from the steady-state spectra.

Kemnitz and Sakaguchi[16] studied the fluorescence kinetics of $H_2TMPyP(4)$ in various solutions. For $H_2TMPyP(4)$ in borate buffer and water these authors found a concentration-dependent, two-exponential fluorescence decay which was attributed to a monomer−dimer equilibrium. Because the fastest component of 1.3 ns increased relative to the slower component of 5.2 ns in buffer (4.9 ns in water) at lower concentrations, they ascribed it to the monomer of $H_2TMPyP(4)$. The same interpretation was published by Brookfield *et al.*,[13] reporting components of 3.7 and 6.1 ns in water for monomer and dimer, respectively. These observations deviate from those of Kano *et al.*[10] who reported a single component of 4.1 ns in water which was ascribed to the dimer of $H_2TMPyP(4)$. Kalyanasundaram[25] reported monoexponential decays in water with lifetimes of 13.8, 7.9, and 6.0 for the tosylate salts of $H_2TMPyP(2)$, $H_2TMPyP(3)$, and $H_2TMPyP(4)$, respectively.

As shown before, we found no evidence for dimerization of $H_2TMPyP(4)$ in water. The two-exponential fluorescence decay can be accounted by the presence of two types of porphyrins: (i) in solution and (ii) adsorbed at the surface of the quartz cuvette. This may explain why some authors observe a single component whereas others observe two components: due to differences in the geometry of the single photon counting setup, fluorescence light originating from porphyrins adsorbed at the sidewalls may or may not reach the detector in experiments of different authors. This explanation is supported by the observation that $H_2TMPyP(2)$ and $H_2TMPyP(3)$ in water and all isomers of H_2TMPyP in methanol give rise to two components for the fluorescence decay (Table 3).

Note also that the long-lived fluorescence component exhibits a marked solvent dependence for $H_2TMPyP(4)$, whereas the shorter lifetime component hardly changes. This difference decreases in the order $H_2TMPyP(4)$ > $H_2TMPyP(3)$ > $H_2TMPyP(2)$. The lifetime-selected spectrum (Figure 6) of the long component resembles the steady-state fluorescence spectrum of H_2TMPyP in solution whereas we attribute the spectrum of the second component to the adsorbed fraction. The concentration dependence of the relative amplitudes of the two components in the fluorescence decay observed by Kemnitz *et al.*[16] can be explained by the high affinity of $H_2TMPyP(4)$ for surfaces. The amount of fluorescent porphyrins adsorbed at the wall or at particles in solution is determined by the constant surface area whereas the amount of porphyrins in solution varies with the concentration. This results in an increasing contribution to the fluorescence of the absorbed porphyrins at decreasing concentration.

The differences in spectroscopic properties between the three isomers should be accounted for by the position of the methyl group at the pyridyl group. To determine the effect of steric hindrance of the different isomers for rotation of the pyridinium group we performed molecular mechanics calculations. The dihedral angles which determine the orientation of the four pyridinium groups with respect to the porphyrin macrocycle were constrained by a harmonic potential with a force constant of 1000 kcal/mol and varied in several conformations between coplanar and perpendicular with steps of 5°. Every conformation was allowed to relax to a local minimum (Figure 7). The results show minimal differences in steric hindrance between $H_2TMPyP(3)$ and $H_2TMPyP(4)$. Their potential energy as a function of the dihedral angle between the planes shows a very shallow double minimum at an angle of ≈25° from the perpendicular orientation. For $H_2TMPyP(2)$ the potential energy is much steeper and shows a single minimum at 0°, due to increased steric hindrance. The latter conclusion agrees with that of Monaco and Zhao,[34] who applied semiempirical molecular orbital calculations (MNDO and AM-1) for $H_2TMPyP(2)$ and $H_2TMPyP(4)$, taking into account (which we did not) the changes in the electronic distribution as a result of twisting one or more pyridinium rings. Their calculations do not give rise to ground-state potentials with shallow double minima, as shown in Figure 7, however. Whereas our calculations admittedly may underestimate the electronic effects, taken into account in Monaco and Zhao's treatment, our molecular mechanics model for the ground state includes dispersive forces, which are absent in the MO calculations. To be sure, the difference in the shape of the potential for both treatments does not affect the essence of the excited-state model, which we propose to explain the different fluorescence properties of the various isomers, since we also approximate the excited-state potential as harmonic (see Discussion).

Discussion

The ^1H NMR results clearly indicate that the ground-state of $H_2TMPyP(4)$ is monomeric in water, but the formation of excimers following excitation cannot be excluded. In aqueous solutions of porphyrins $\leq 1 \times 10^{-4}$ M, the fraction of excimers formed can be calculated to be negligibly small if we assume a monomeric fluorescence lifetime of 10 ns and a diffusion constant of 1.1×10^{-10} m^2s^{-1}. Our data show that the use of the concentration dependence of the fluorescence spectra by Kano *et al.*[9-11,14] as the main argument for the presence of "loose dimers" which form excimers following excitation cannot be maintained. It is rather the presence of traces of solid material present even in purified water which determines the porphyrin upper limit concentration, at which the fluorescence spectra show increased resolution. Also, the fluorescence kinetics of $H_2TMPyP(4)$, explained by a monomer−dimer equilibrium by Brookfield *et al.*[13] and Kemnitz *et al.*,[16] can alternatively be attributed to the affinity of $H_2TMPyP(4)$ to the inner surface of the quartz cuvettes. Furthermore, the presence of adsorbed and dissolved porphyrins offers an explanation for the fluorescence kinetics of both $H_2TMPyP(2)$ and $H_2TMPyP(3)$ in water and all isomers in apolar solution. The changes observed in the fluorescence spectrum of $H_2TMPyP(3)$ and $H_2TMPyP(4)$ and to a lesser extent of $H_2TMPyP(4)$, upon a change of temperature or solvent polarity, must therefore be explained by an *intramolecular* mechanism.

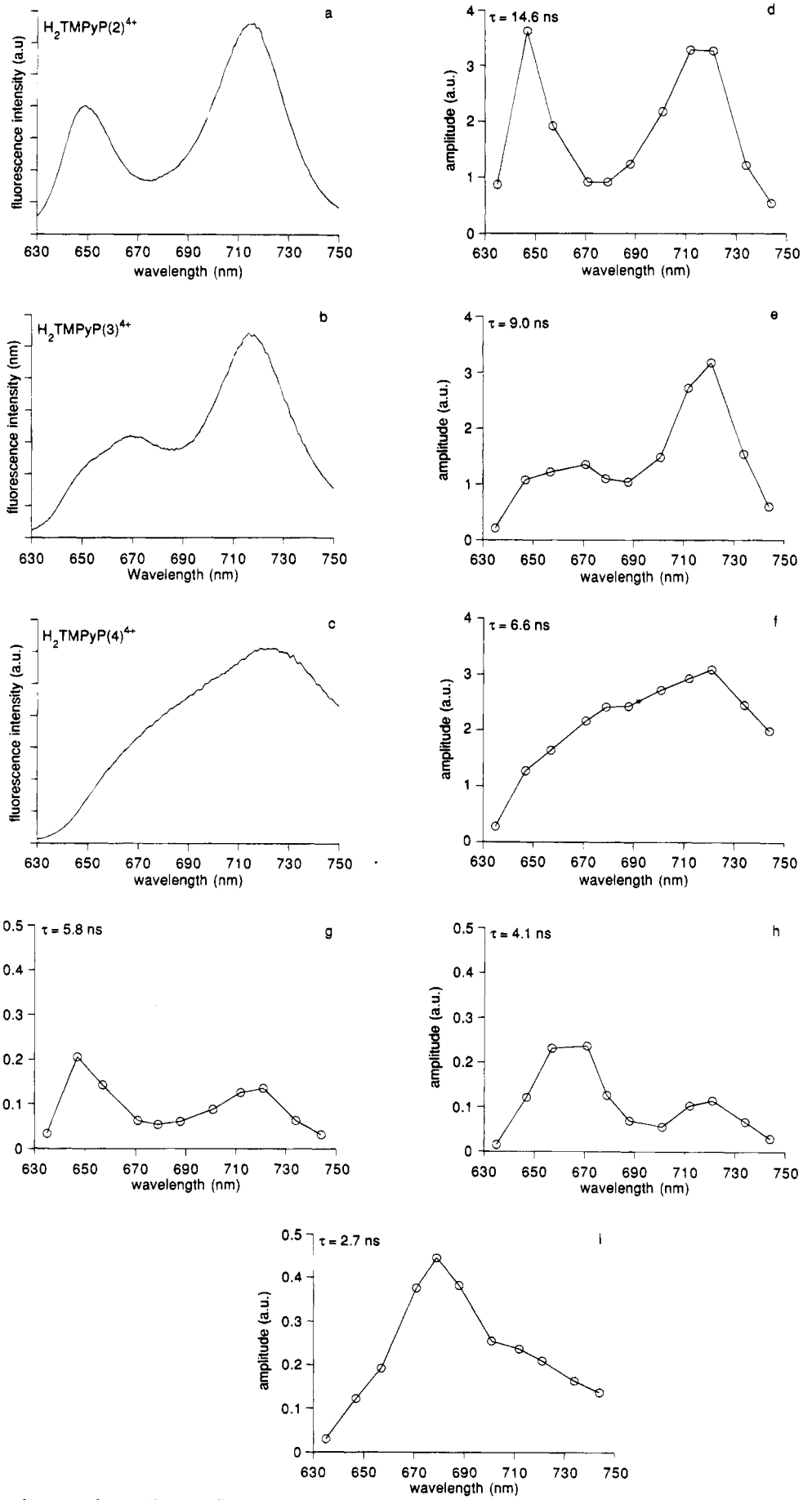

Figure 6. Comparison between the steady-state fluorescence spectra of the three isomers of H_2TMPyP in water (a–c) and the lifetime-selected spectra of the two main components in the fluorescence lifetime decays (d–i): (a, d, and g) $H_2TMPyP(2)$; (b, e, and h) $H_2TMPyP(3)$; (c, f, and i) $H_2TMPyP(4)$.

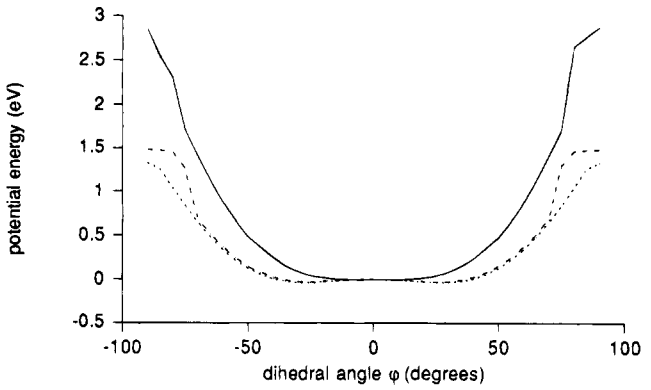

Figure 7. Excited-state potentials for the three isomers of H_2TMPyP as a function of the dihedral angle φ between the porphyrin plane and the pyridinium group: (—) $H_2TMPyP(2)$; (– –) $H_2TMPyP(3)$; (- - -) $H_2TMPyP(4)$.

Several properties of porphyrins, e.g., absorption and fluorescence spectra, redox potentials, basicity, and kinetics for proton uptake of free base porphyrins, have a strong dependence on the type and position of substituents attached at the meso position or to the pyrrole rings. These effects have been explained using the electron-accepting or -donating properties of substituents as well as steric effects. According to Gouterman's four-orbital model,[35-38] for free base tetraphenylporphyrin substituents at the methine position of the porphyrin macrocycle affect the energy of the a_{2u} orbital but not of the a_{1u} orbital. This causes a change in configuration interaction and thus of the position and intensity of the Q transitions. The Q(0,0) bands are more affected then the Q(0,1) bands due to vibronic coupling.

The effect of the electron-accepting pyridinium groups on the visible spectra can be noted in both the absorption and the fluorescence spectra of the three isomers of H_2TMPyP by a smaller Q(0,0)/Q(0,1) ratio as compared to that for H_2TPP. Although the absorption spectra of the three isomers do not show noticeable variations, the fluorescence spectra exhibit distinct differences, suggesting different intramolecular interactions in the excited state as compared to those in the ground state. This suggestion is confirmed by the absence of a temperature effect in the absorption spectra contrary to the clear temperature effect in the fluorescence spectra (see Figure 5).

The electron-accepting effect of the pyridinium groups has both an inductive and a mesomeric character. The inductive effect propagates via the σ-bonds of the pyridinium group toward the porphyrin σ-system and therefore does not influence the energy of the π-orbitals. The effect decreases with a factor 3 per C–C bond. Any inductive electron-accepting effect is expected to increase in the order $H_2TMPyP(4) < H_2TMPyP(3) < H_2TMPyP(2)$. The mesomeric effect propagates via the π-system and reflects the possible resonance structures of the isomers, implying that for this mechanism only ortho and para substitution of the pyridinium group, but much less meta substitution, affects the electronic structure of the porphyrin core directly. For the meta-substituted pyridinium group only an indirect mesomeric effect via the C atoms neighboring the N atom is expected.

Resonance interaction between the π-system of the porphyrin macrocycle and the pyridinium group requires a rotation toward a coplanar conformation. The pyridinium methyl group is sterically hindered by the porphyrin pyrrole rings for $H_2TMPyP(2)$, limiting resonance interaction between both ring systems. It is clear that the strongest mesomeric effect is predicted for $H_2TMPyP(4)$. The order for $H_2TMPyP(2)$ and $H_2TMPyP(3)$ is less clear. The mesomeric electron-accepting effect, taking into account differences in steric hindrance between $H_2TMPyP(2)$ and $H_2TMPyP(4)$, is expected to increase in the series $H_2TMPyP(3) < H_2TMPyP(2) < H_2TMPyP(4)$. The reasoning to predict the order of influence for the three isomers of the inductive and mesomeric effect includes the assumption of total localization of the positive charge of the pyridinium group on the quaternized nitrogen.

For aqueous solutions the longest fluorescence lifetime component decreases in the series $H_2TMPyP(2) > H_2TMPyP(3) > H_2TMPyP(4)$ with a lifetime for the ortho isomer close to that for unsubstituted tetraphenylporphyrin. The same order is found for the effect of decreasing polarity or increasing temperature on the resolution of the fluorescence spectrum. This order in substituent effect ($H_2TMPyP(4) > H_2TMPyP(3) > H_2TMPyP(2)$) is not in accordance with any of the above-mentioned predictions.

A model is presented which can explain the salient experimental results. First, we note that the energy of the intramolecular CT state, for which an electron is fully transferred, following optical excitation, from the porphyrin macrocycle to the pyridinium group, is close to the locally excited singlet state S_1. From the oxidation potential of free base porphin ($\approx$1.0 V vs NHE) and the reduction potential of *N*-methylpyridinium, the energy of this CT state in polar solvents can be estimated.[39] For *N*-methylpyridinium we used the reduction potential of 3,3′-bis-(*N*-methylpyridinium) (≈ -1.0 V vs NHE),[40] which can be considered as a molecule with two weakly interacting *N*-methylpyridinium units. Using this assumption the energy of the CT state is calculated as $\approx$2.0 eV, almost equal to the S_1 energy (1.9 eV). Because of the near-degeneracy of the S_1 and CT states, mixing may readily occur by vibronic coupling, with the pyridinium librational vibration as the active mode. Mixing of the S_1 and a CT state with higher energy, resulting in increased radiationless decay of the excited porphyrin, was already suggested for orthogonal porphyrin π-systems by Wasielewski *et al.*[41] to explain their fluorescence data.

The model assumes that the potential energy curves of the unperturbed localized excited state (S_1^0) and the unperturbed CT state (CT^0) as a function of the dihedral angle $-90° < \varphi < 90°$ between the porphyrin plane and the normal to the plane of the pyridinium group is equal to that calculated for the ground state by molecular mechanics. Although this is certainly incorrect for the skeletal vibrations of the ground and excited states of the porphyrin core in view of the relative intensities of the fluorescence 0–0 and 0–1 vibronic transitions, this assumption seems reasonable when considering the pyridinium librational mode, since (i) the equilibrium value of φ in the S_1^0 as well as the CT^0 state of the free molecule at room temperature must be equal to that in the ground state; i.e., the average value of $\varphi = 0$ for each of these states; (ii) the excitation in the S_1^0 state is localized on the porphyrin macrocycle, only indirectly affecting the excited-state librational potential $V^*(\varphi)$, e.g., by a fractional change of the π-electron density on the methine groups of the porphyrin macrocycle, resulting in a relatively small change of the barrier height for the pyridinium librational motion; (iii) the net + and − charges are the result of a $\pi \rightarrow \pi$ transition from the porphyrin macrocycle to the pyridinium group, again affecting only the π-electron densities on the groups contributing to the barrier height, the porphyrin methine carbon, and the pyridinium ortho-carbon. Also for the CT^0 state, the fractional change of the π-electron density on these groups is not expected to have a large effect on the angular dependence of the electronic coupling matrix element $H_{12}(\varphi) = H_{21}(\varphi) = \epsilon(\varphi)$ between the nonhybridized $2p_z$ orbitals of the porphyrin methine carbon and the adjacent pyridinium

carbon which has been modeled by $\epsilon \sin^2(\varphi)$. The effective potentials $V_\pm$ of the perturbed S_1^0 and CT^0 states are then given by

$$V_\pm = {}^1/_2[E(S_1^0) + E(CT^0)] + V_\pm(\varphi) \pm {}^1/_2[(\Delta E)^2 + 4\epsilon^2 \sin^4(\varphi)]^{1/2} \quad (3)$$

where $V_0(\varphi)$ is the ground-state potential calculated by molecular mechanics, $E(S_1^0)$ and $E(CT^0)$ are the energies of the unperturbed S_1^0 and CT states, with ΔE their difference. Note that ΔE is independent of φ.

Ignoring the shallow minima, $V_0(\varphi)$ and $V^*(\varphi)$ can be approximated by harmonic potentials $V_0(\varphi) = V_0\varphi^2$ and $V^*(\varphi) = V^*\varphi^2$, respectively. Due to the interaction between the S_1^0 and CT states $V^*_- < V_0$, whereas $V^*_+ > V_0$. The rms width $\Delta\varphi$ of the $S^*_{1,\nu=0}$ librational wavefunction is given by

$$\Delta\varphi = 2[\hbar^2/(2V_0I)]^{1/4} \quad (4)$$

with I the moment of inertia of the pyridyl group. Inserting the calculated values of V_0 for the three isomers, it follows from (3) that V^*_- decreases and therefore $\Delta\varphi$ increases in the order $H_2TMPyP(4) > H_2TMPyP(3) > H_2TMPyP(2)$. Assuming that emission occurs from the $\nu = 0$ librational state, an increase of its rms width results in a broadening of the $S^*_{1,0} \rightarrow S_{1,\nu=0}$ fluorescence emission for TMPyP(4) as compared to that for the other two isomers, due to the larger number of accessible, close-lying S_0 librational states of the para-substituted isomer $H_2TMPyP(4)$. Concluding, the different broadening of the fluorescence spectra of the three isomers reflects their relative increase in the librational amplitude in the perturbed excited singlet state. This increase is largest for the least sterically hindered pyridinium group. This is most clearly seen in the lifetime selected fluorescence spectra for desolved (Figure 6d−f) and the absorbed species (Figure 6g−i). The effects of solvent polarity is most pronounced for Figure 6d−f and less for Figure 6g−i.

ΔE in (2) increases if the dielectric constant of the solvent is decreased, thus destabilizing the CT state. Then, the effect of the electronic coupling between the unperturbed S_1 and CT states is reduced, and the spectral broadening should disappear, in agreement with the effect of substituting water by methanol as a solvent (Figure 2). Whether the return to a resolved fluorescence spectrum upon adsorption on a solid surface is due to immobilization of the pyridinium groups or to a different polarity of the surface as compared to the solution cannot be explained from our experiments.

The behavior of the present system remotely resembles that of a TICT state.[42] Note, however, that contrary to what is usually observed for such a state, for the porphyrins in this work the interaction between the rotating side groups and the porphyrin core increases, rather than decreases, upon excitation.

To gain more insight in the spectral changes observed as a function of polarity and temperature we analyzed the fluorescence spectra of the three isomers. All fluorescence spectra can be fitted to a sum of Gaussians. To compare the effects of temperature and polarity we plotted the parameters describing the Gaussians as a function of the dielectric constant of the solvents. From this comparison we conclude that the effects of changes in temperature on the fluorescence spectra are in fact due to changes in solvent polarity with temperature. The effect of polarity on the fluorescence spectra decreases in the series $H_2TMPyP(4) > H_2TMPyP(3) > H_2TMPyP(2)$. In addition the parameters describing the spectra for the three isomers become more alike in methanol.

The difference in fluorescence yield between the iodide and the chloride salts in methanol ($\epsilon_r = 32.6$) (Figure 4), which is not found for the fluorescence lifetime, can be explained by static quenching, due to the external heavy atom effect on the intersystem crossing. Note that the iodide ion is heavier then the chloride ion, so a larger effect is expected in the iodide salt than in the chloride salt when the ions are close to the excited porphyrin, as in methanol. In water the Cl^- and I^- ions are completely dissociated from the porphyrin moiety, so there is no appreciated effect on the intersystem crossing at the concentrations we use in out experiments. The increase of the fluorescence yield upon adding methanol to the aqueous solution ($70 < \epsilon_r < 82$) is the result of the demixing of the CT and S_1 states unperturbed.

Raman excitation profiles and lifetime measurements on CuTMPyP(4) have suggested that poly(dA-dT) traps a significantly distorted Q-excited state,[23] prior to the formation of the TMPyP−porphyrin−DNA exciplex, which is thought to be responsible for the photoinduced DNA strand-breaking. These studies have not made clear, however, whether the distortion of the porphyrin is an intrinsic property of its excited state or is primarily induced by its interaction with DNA. This work provides further evidence for a distorted intramolecular exciplex for porphyrins without axial ligands, even in the absence of additional electron acceptors. The exciplex formation in CuTMPyP complexes with a variety of oligo- and polynucleotides has been explained by a different mechanism, i.e., by photoinduced axial ligation,[22,24] and is not in conflict with our results.

Conclusions

We have provided evidence that the ortho-, meta-, and para-substituted isomers of H_2TMPyP^{4+} are monomeric in water below 10^{-3} M. Mixing of the S_1 and a close-lying CT state in which an electron is transferred from the porphyrin core to a pyridinium group causes a reduction in fluorescence lifetime and rather large changes in fluorescence spectra as a function of the solvent polarity. The amount of mixing is determined by the degree of freedom to reach coplanarity of the π-systems ($H_2TMPyP(4) \approx H_2TMPyP(3) > H_2TMPyP(2)$) and by solvent polarity. When sterically possible, rotation of the pyridinium groups increases the electronic mixing between the S_1 and the energetically nearby CT state by a conformational change, involving the libration of the pyridinium group as the active mode for vibronic mixing of the electronic states.

Acknowledgment. This investigation was supported by the Netherlands Foundation for Chemical Research (SON) with financial aid of the Netherlands Organisation for Scientific Research (NWO). The authors thank Mr. A. van Veldhuizen of the Department of Organic Chemistry, Wageningen, for running the ^1H NMR spectra.

References and Notes

(1) Vergeldt, F. J.; Koehorst, R. B. M.; Schaafsma, T. J.; Lambry, J. C.; Martin, J. L.; Johnson, D. G.; Wasielewski, M. R. *Chem. Phys. Lett.* **1991**, *182*, 107.

(2) Segawa, H.; Takehara, C.; Honda, K.; Shimidzu, T.; Asahi, T.; Mataga, N. *J. Phys. Chem.* **1992**, *96*, 503.

(3) Tran-Thi, T. H.; Lipskier, J. F.; Houde, D.; Pepin, C.; Keszei, E.; Jaygerin, J. P. *J Chem. Soc., Faraday Trans.* **1992**, *88*,

(4) Hofstra, U.; Koehorst, R. B. M.; Schaafsma, T. J. *Magn. Reson. Chem.* **1987**, *25*, 1069.

(5) Goodwin, J. A.; Scheidt, W. R. *J. Phys. Chem.* **1990**, *94*, 4432.

(6) Pasternack, R. F.; Huber, P. R.; Boyd, P.; Engasser, G.; Francesconi, L.; Gibbs, E.; Fasella, P.; Venturo, G. C.; Hinds, L. d. *J. Am. Chem. Soc.* **1972**, *94*, 4511.

(7) Pasternack, R. F. *Ann. N. Y. Acad. Sci.* **1973**, *206*, 614.

(8) White, W. I. In *The Porphyrins* ; Dolphin, D., Eds; Academic Press: New York, 1978; p 303.
(9) Kano, K.; Takei, M.; Hashimoto, S. *J. Phys. Chem.* **1990**, *94*, 2181.
(10) Kano, K.; Miyake, T.; Uomoto, K.; Sato, T.; Ogawa, T.; Hashimoto, S. *Chem. Lett.* **1983**, 1867.
(11) Kano, K.; Sato, T.; Yamada, S.; Ogawa, T. *J. Phys. Chem.* **1983**, *87*, 566.
(12) Pasternack, R. F.; Gibbs, E. J.; Gaudemer, A.; Antibe, A.; Bassner, S.; Poy, L. D.; Turner, D. H.; Williams, A.; Laplace, F.; Lansard, M. H.; Merienne, C.; Perree-Fauvet, M. *J. Am. Chem. Soc.* **1985**, *107*, 8179.
(13) Brookfield, R. R.; Ellul, H.; Harriman, A. *J. Photochem.* **1985**, *31*, 97.
(14) Kano, K.; Nakajima, T.; Takei, M.; Hashimoto, S. *Bull. Chem. Soc. Jpn.* **1987**, *60*, 1281.
(15) Kadish, K. M.; Maiya, B. G.; Araullo-McAdams, C. *J. Phys. Chem.* **1991**, *95*, 427.
(16) Kemnitz, K.; Sakaguchi, T. *Chem. Phys. Lett.* **1992**, *196*, 497.
(17) Hambright, P.; Fleischer, E. B. *Inorg. Chem.* **1970**, *9*, 1756.
(18) Fiel, R. J.; Datta-Gupta, N.; Mark, E. H.; Howard, J. C. *Cancer Res.* **1981**, *41*, 354.
(19) Carvlin, M. J.; Fiel, R. *Nucleic Acids Res.* **1983**, *11*, 6121.
(20) Carvlin, M. J.; Mark, E.; Fiel, R. *Nucleic Acids Res.* **1983**, *11*, 6141.
(21) Kelly, J. M.; Murphy, M. J.; McConnell, D. J.; OhUigin, C. *Nucleic Acids Res.* **1985**, *13*, 167.
(22) Turpin, P.-Y.; Chinsky, L.; Laigle, A.; Tsuboi, M.; Kincaid, J. R.; Nakamoto, K. *Photochem. Photobiol.* **1990**, *51*, 519.
(23) Chinsky, L.; Turpin, P.-Y.; Al-Obaidi, A. H. R.; Bell, S. E. J.; Hester, R. E. *J. Phys. Chem.* **1991**, *95*, 5754.
(24) Mojzes, P.; Chinsky, L.; Turpin, P.-Y. *J. Phys. Chem.* **1993**, *97*, 4841.
(25) Kalyanasundaram, K. *Inorg. Chem.* **1984**, *23*, 2453.
(26) 'Conner, D. V.; Philips, D. *Time-Correlated Single Photon Counting*; Academic Press Inc.: London, 1987.
(27) Hoek, A. v.; Visser, A. J. W. G. *Rev. Sci. Instrum.* **1981**, *52*, 1199.
(28) Livesey, A. K.; Bronchon, J. C. *Biophys. Bioeng.* **1987**, *13*, 105.
(29) Beechem, J. M.; Gratton, E. *Proc. SPIE* **1988**, *909*, 70.
(30) Beechem, J. M.; Gratton, E.; Ameloot, M.; Knutson, J. R.; Brand, L. In *Topics in Fluorescence Spectroscopy*; Lakowicz, J. R., Eds; Plenum Press: New York, 1991; p 241.
(31) Abraham, R. J.; Smith, K. M.; Goff, D. A.; Lai, J. *J. Am. Chem. Soc.* **1982**, *104*, 4332.
(32) Koehorst, R. B. M.; Hofstra, U.; Schaafsma, T. J. *Magn. Reson. Chem.* **1988**, *26*, 167.
(33) Jortner, J. J. *Proc. Natl. Acad. Sci. U.S.A.* **1974**, *71*, 3640.
(34) Monaco, R. R.; Zhao, M. *Int. J. Quantum Chem.* **1993**, *46*, 701.
(35) Gouterman, M. *J. Chem. Phys.* **1959**, *30*, 1139.
(36) Gouterman, M. *J. Mol. Spectrosc.* **1961**, *6*, 138.
(37) Gouterman, M.; Wagniere, G. H.; Snyder, L. C. *J. Mol. Spectrosc.* **1963**, *11*, 108.
(38) Meot-Ner, M.; Adler, D. *J. Am. Chem. Soc.* **1975**, *97*, 5107.
(39) Weller, Z. Z. *Phys. Chem.* **1982**, *133*, 93.
(40) Bard, A. J.; Lund, H. *Derivatives of Ammonia. Heteroaromatic compounds*; Marcel Dekker Inc.: New York, 1984.
(41) Wasielewski, M. R.; Johnson, D. G.; Niemczyk, M. P.; Gaines, G. L. I.; O'Neil, M. P. *J. Am. Chem. Soc.* **1990**, *112*, 6482.
(42) Rettig, W. *Angew. Chem. Int. Ed. Engl.* **1986**, *25*, 971.
(43) Åkerlöf, G. *J. Am. Chem. Soc.* **1932**, *54*, 4125.

JP941206N